Calculations of output power of the graphene-based terahertz laser

O.N. Kozina
Saratov Branch
Kotel’nikov Institute of Radio-Engineering and Electronics of Russian Academy of Science
Saratov, Russia
kozinaolga@yandex.ru

L.A. Melnikov
Department of Instrumentation Engineering
Yuri Gagarin State Technical University of Saratov
Saratov, Russia

I.S. Nefedov
School of Electrical Engineering
Aalto University,
Aalto, Finland

Aalto University
School of Electrical Engineering

Terahertz lasing

Approaches:
Enhancement interaction between incoming photons and free carriers in graphene by arrays of resonant nanocavities in form of a periodic graphene strip line;
Idea of the Salisbury absorber - to place a metal screen at quarter-wave distance from the graphene layer.

Otsuji, T.; Popov, V.; Ryzhii, V. Active graphene plasmonics for terahertz device applications. J. Phys. D Appl. Phys. 2014, 47, 094006 .
Ying X, Pu Y, Luo Y, Peng H, Li Z, Jiang Y, Xu J and Liu Z 2017 Enhanced universal absorption of graphene in a Salisbury screen J. Appl. Phys. 121 023110

The disadvantage of approaches and similar implementations is an interaction with a single graphene layer that restricts a power of amplified radiation due to a small volume of a light-matter interaction

Hyperbolic metamaterials (HMM)

Multilayer periodic structure composed of graphene layers possess hyperbolic properties at THz region

I.V. Iorsh, I.S. Mukhin, I.V. Shadrivov, P.A. Belov, Y.S. Kivshar, "Hyperbolic metamaterials based on multilayer graphene structures," Phys. Rev. B, vol. 87, p. 075416, 2013.

Alternative approach for realization of the THz amplification –
graphene-based asymmetric hyperbolic metamaterial (AHMM)

Nefedov I., Melnikov L. Plasmonic terahertz ampli_cation in graphene-based asymmetric hyperbolic metamaterial. Photonics 2015, 2, 594-603, 2015
O.N. Kozina, L.A. Melnikov, I.S. Nefedov, "Dispersion characteristics of hyperbolic graphene-semiconductors multilayered structure," in Proceedings of SPIE, vol. 9448, Article CID 9448-11, N. 9448-108, 2015.
Nefedov, I.S.; Valagiannopoulos, C.A.; Melnikov, L.A. Perfect absorption in graphene multilayers. J. Opt. 2013, 15, 114003. 2013.

Cavity partially filled with AHMM

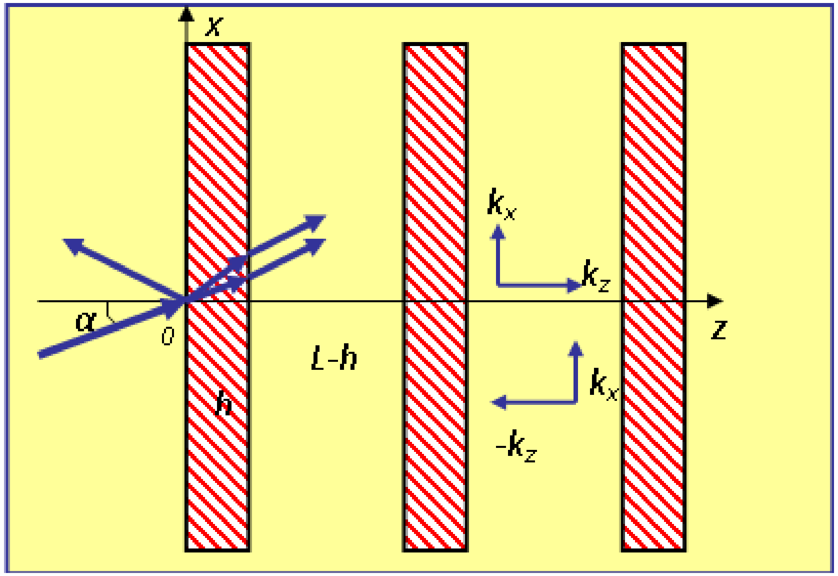

Rectangle – AHMM
Red planes symbolized graphene sheets

Total round-trip transfer matrix

$$P_t = P_0(l_1 + l_2)P(h)$$

$\boldsymbol{P_t}$ - determine the gain and phase delay of the corresponded eigenwaves at one pass

$\boldsymbol{\Lambda_{i,k}}$=exp($i\kappa_{i,k}L$) - eigenvalues of $\boldsymbol{P_t}$

$\boldsymbol{\Lambda_{i,k}}$ - characterizes the phase delay at one pass ($L=l_1+l_2+h$).

Re[$\varkappa_{i,k}$]=2πm, condition, gives the oscillation frequency of the laser

A cavity partially filled with AHM slab is modelled as an infinite number of AHM slabs, periodically placed in the isotropic lossy medium (yellow area).

Wave vectors of eigenwaves are shown schematically by dark blue arrows.

Cavity modes are eigenwaves of this structure.

Asymmetric Hyperbolic Metamaterials (AHMM)

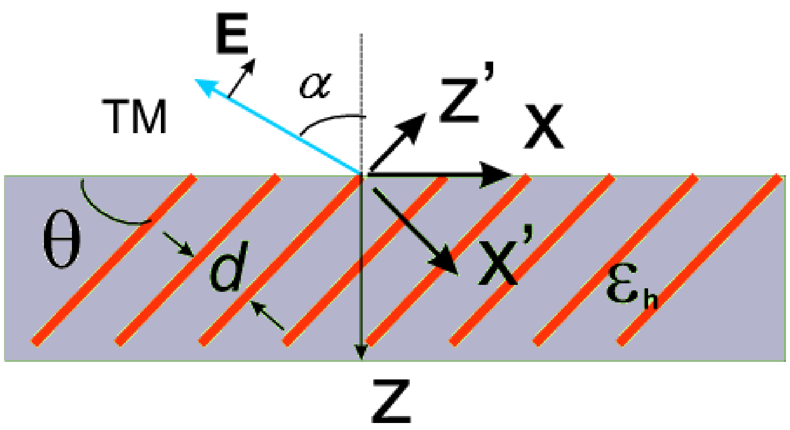

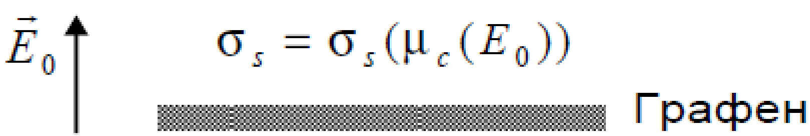

$$\bar{\varepsilon} = \begin{bmatrix} \varepsilon_{\parallel} & 0 & 0 \\ 0 & \varepsilon_{\perp} & 0 \\ 0 & 0 & \varepsilon_{\perp} \end{bmatrix}$$

$$\varepsilon_{\parallel} = \varepsilon_h = \varepsilon_{SiC}$$

$$\varepsilon_{\perp} = \varepsilon_{\parallel} + i\frac{\sigma(\omega)}{d\omega\varepsilon_0}$$

$$\varepsilon_{\perp} = \varepsilon_{\parallel} + \frac{i}{d\omega\varepsilon_0}\left[\sigma'(\omega, E_0) + i\sigma''(\omega, E_0)\right]$$

$$\sigma(\omega, E_0) = \sigma_{intra} + \sigma_{inter}$$

Г. С. Макеева, О. А. Голованов, В. В. Вареница, Д. В. Артамонов
Физико-математические науки. Физика. № 3 (31), 2014

Permittivity of SiC

$$\varepsilon_k(\omega) = \varepsilon_{k\infty} + \frac{\omega_{kp}^2}{\omega_{kTO}^2 - \omega^2 - i\gamma_k\omega}$$

$$\omega_{kp}^2 = \varepsilon_{k\infty}(\omega_{kLO}^2 - \omega_{kTO}^2)$$

$$k = p, t$$

$$\varepsilon_{SiC} = \frac{\varepsilon_{k=p} + \varepsilon_{|k=t}}{2}$$

H. Mutschke, A.C. Andersen, D. Cl.ement, Th. Henning, G. Peiter, Astron. Astrophys. 345, 187–202 (1999).

Kubo model of conductivity

$$\sigma_{gr}(\omega) = \left(\frac{e^2}{4\hbar}\right)\frac{8k_BT\tau}{\pi\hbar(1 - i\omega\tau)}\ln\left[1 + \exp\left(\frac{E_F}{k_BT}\right)\right]$$
$$+\left(\frac{e^2}{4\hbar}\right)\tanh\left(\frac{\hbar\omega - 2\varepsilon_F}{4k_BT}\right)$$
$$-\left(\frac{e^2}{4\hbar}\right)\frac{4\hbar\omega}{i\pi}\int_0^{\infty}\frac{G(E, E_F) - G(\hbar\omega/2, E_F)}{(\hbar\omega)^2 - 4E^2}dE$$

Hanson G. W., J. Appl. Phys. 103 064302 (2008)

AHMM.
Method Berreman 4x4 matrix

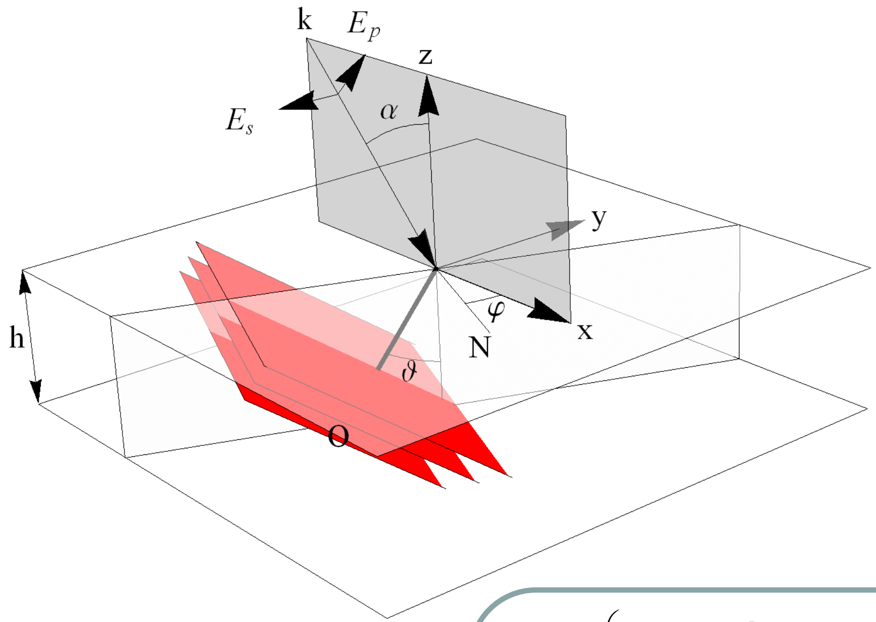

$$\frac{\partial}{\partial z}\Psi = \frac{i\omega}{c}\Delta\Psi$$

$$\Psi = \begin{pmatrix} E_x \\ H_x \\ E_y \\ -H_y \end{pmatrix}$$

$\Psi\exp(ikr\text{-}i\omega t)$

$k=(kx,ky,kz)$

$K = \omega/c = 2\pi/\lambda$

h – thickness of AHMM

α- incidence angle

θ, φ, ψ - Euler's angles,

N - line of nodes

$\psi=0$

$$\Delta = \begin{pmatrix} -\frac{k_x}{K}\frac{\varepsilon_{zx}}{\varepsilon_{zz}} & 1-\left(\frac{k_x}{K}\right)^2\frac{1}{\varepsilon_{zz}} & -\frac{k_x}{K}\frac{\varepsilon_{zy}}{\varepsilon_{zz}} & -\left(\frac{k_x}{K}\right)\left(\frac{k_y}{K}\right)\frac{1}{\varepsilon_{zz}} \\ \varepsilon_{xx}-\frac{\varepsilon_{zx}\varepsilon_{xz}}{\varepsilon_{zz}}-\left(\frac{k_y}{K}\right)^2 & -\frac{k_x}{K}\frac{\varepsilon_{xz}}{\varepsilon_{zz}} & \varepsilon_{xy}-\frac{\varepsilon_{zy}\varepsilon_{xz}}{\varepsilon_{zz}}+\left(\frac{k_x}{K}\right)\left(\frac{k_y}{K}\right) & -\frac{k_y}{K}\frac{\varepsilon_{xz}}{\varepsilon_{zz}} \\ -\frac{k_y}{K}\frac{\varepsilon_{zx}}{\varepsilon_{zz}} & -\left(\frac{k_x}{K}\right)\left(\frac{k_y}{K}\right)\frac{1}{\varepsilon_{zz}} & -\frac{k_y}{K}\frac{\varepsilon_{zy}}{\varepsilon_{zz}} & 1-\left(\frac{k_y}{K}\right)^2\frac{1}{\varepsilon_{zz}} \\ \varepsilon_{yx}-\frac{\varepsilon_{yz}\varepsilon_{zx}}{\varepsilon_{zz}}+\left(\frac{k_x}{K}\right)\left(\frac{k_y}{K}\right) & -\frac{k_x}{K}\frac{\varepsilon_{yz}}{\varepsilon_{zz}} & \varepsilon_{yy}-\frac{\varepsilon_{yz}\varepsilon_{zy}}{\varepsilon_{zz}}-\left(\frac{k_x}{K}\right)^2 & -\frac{k_y}{K}\frac{\varepsilon_{yz}}{\varepsilon_{zz}} \end{pmatrix}$$

$\mathbf{k}=(k_x, k_y, k_z)$

$$\Psi_T = \mathbf{P}(h)(\Psi_I + \Psi_R)$$

Berreman D. W., Journal of the Optical Society of America, 62(4), 1157-1160 (1972).
Palto S. P., Journal of Experimental & Theoretical Physics 92(4), 552-562 (2001).
D. A. Yakovlev, V. G. Chigrinov, Modeling and optimization of the LCD optical performance (Hoi-Sing Kwok. Wiley. United Kingdom, 2015

Eigenvalues $\varkappa_{i,k}$ vs k_z

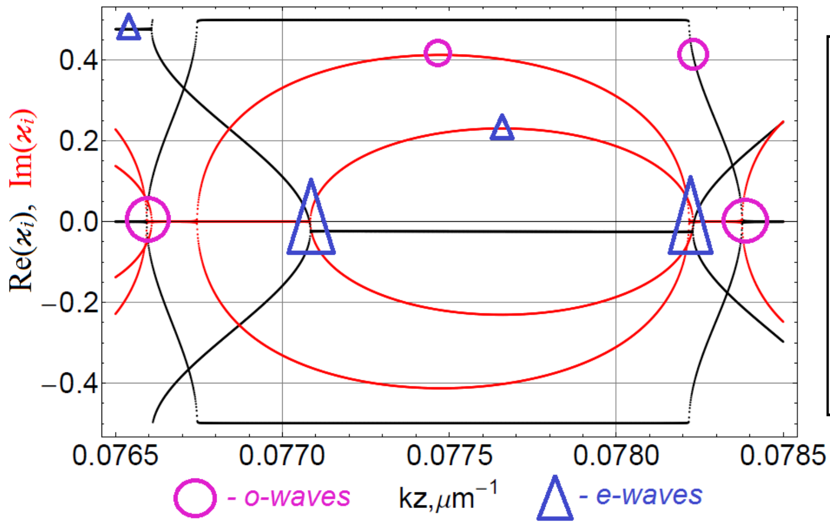

Black – Re($\varkappa_{i,k}$)
Red – Im($\varkappa_{i,k}$)

$\varkappa_{1,2}$ - ordinary waves - solid curves

$\varkappa_{3,4}$ - extraordinary waves - dotted curves

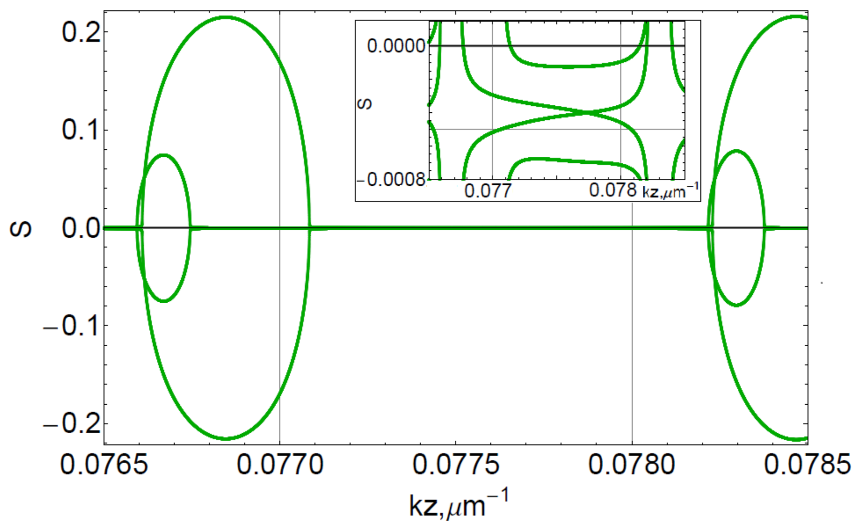

Only waves with
$|\varkappa_{i,k}|>1$, $S_z>0$ or $|\varkappa_{i,k}|<1$, $S_z<0$
are experienced net gain

l_1=600μm,
l_2=1320μm
h=5μm
$\varphi=\pi/2$
θ= 55°
α=15°

z-component of Pointing vector S_z

Saturation

$$\varepsilon_{\perp} = \varepsilon_{\parallel} + \frac{i}{d\omega\varepsilon_0}\left[\sigma'(\omega, E_0) + i\sigma''(\omega, E_0)\right]$$

E_0 is a component of the external electric strength vector transverse to the graphene plane

$$E_0 = \frac{e}{\pi\hbar^2 v_F^2 \varepsilon_b}\int_0^{\infty} d\varepsilon\left(f_d(\varepsilon) - f_d(\varepsilon + 2\mu_c)\right)$$

$f_d(\varepsilon)$ – the Fermi-Dirac function
μ_c – the chemical potential
ε_b – the dielectric constant of graphene

The function $f_d(\varepsilon)$ is determined by $f_d(\varepsilon) = 1/(\exp[\frac{\varepsilon - \mu_c}{k_B T}] + 1)$

Г. С. Макеева, О. А. Голованов, В. В. Вареница, Д. В. Артамонов. // Физико-математические науки. Физика. № 3 (31), 2014
J. B. Khurgin. Graphene—A rather ordinary nonlinear optical material. Appl. Phys. Lett. 104, 161116 (2014);
S. A. Mikhailov. Comment on “Graphene—A rather ordinary nonlinear optical material. Appl. Phys. Lett. 111, 106101 (2017);
Jacob B. Khurgin. Response to “Comment on ‘Graphene—A rather ordinary nonlinear optical material’” [Appl. Phys. Lett. 111, 106101 (2017)]. Appl. Phys. Lett. 111, 106102 (2017)

The dependence of chemical potential (meV) of graphene from transverse electric field (V/nm)

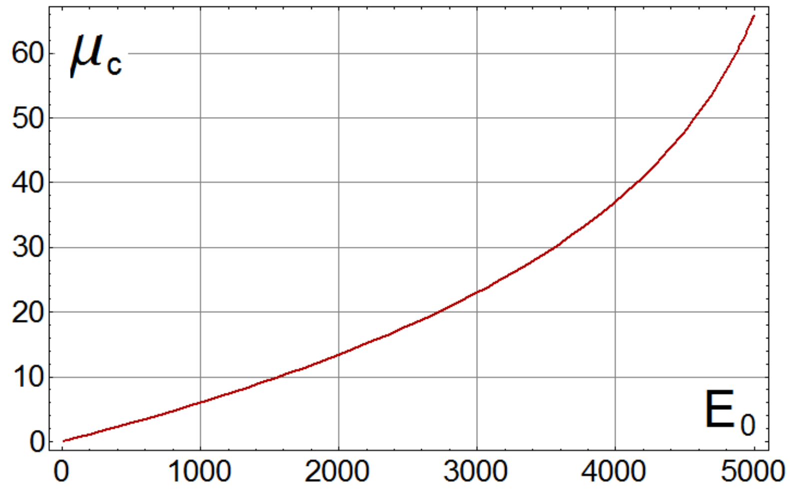

Spectral dependence of the dynamic conductivity of graphene $\sigma_{gr}(\omega,\mu_c(E_0))$

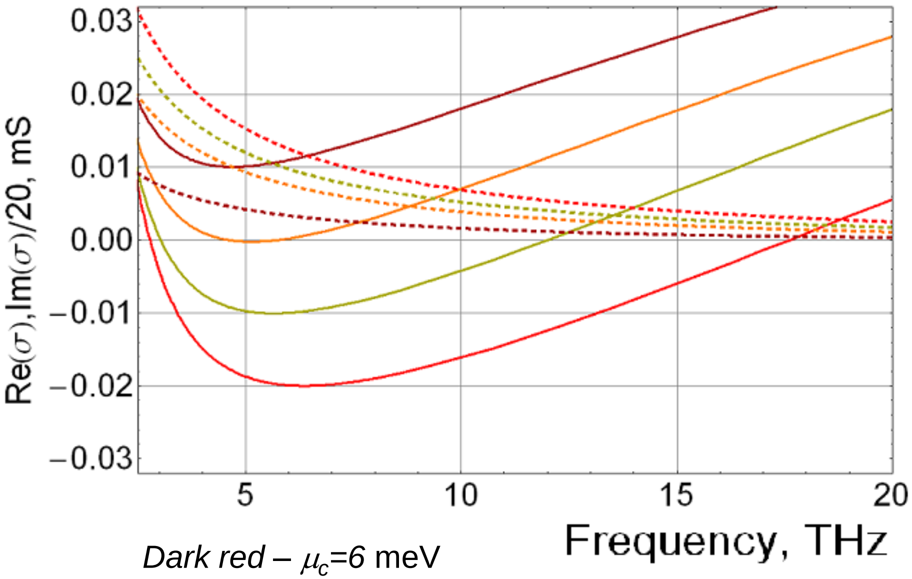

Dark red – μ_c=6 meV
Orange – μ_c=16.2 meV
Yelow – μ_c=26 meV
Red – μ_c=37 meV

Im(ϰ) vs chemical potential (meV) of grapheme

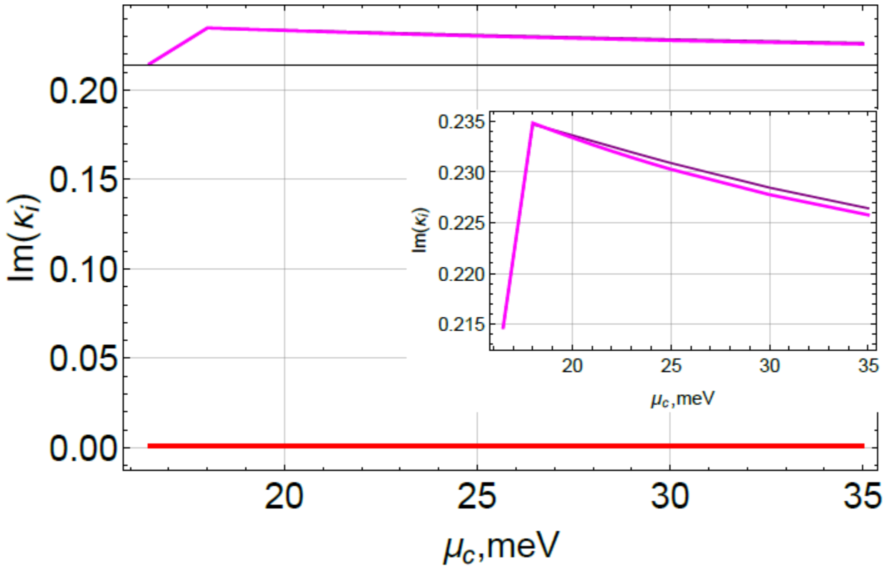

Intensity of THz radiation is about 1.2 10^{15} W/m^2 for the frequencies about 3-4 THz.

Expected THz radiation field strength is about 3.5 10^3 V/nm

and $E_0 \approx 2.7\ 10^{12}$ V/nm.

Conclusion

The iterative theory of single mode THz wave lasing in the cavity with asymmetric hyperbolic active media is presented:

- Both forward and backward waves in the AHMM were included, this gives possibilities to include other than standing wave cavity configurations.
- The frequency of oscillation and field intensity was calculated from the solution of equations for real and imaginary parts of log of eigenvalues of total transfer matrix of one period of the structure.
- The eigenwaves of the cavity at THz frequencies is calculated, accounting the saturation of the gain.